

ORIGINAL ARTICLE: BIOLOGY

Binding and safety profile of novel benzoxazole derivative for *in vivo* imaging of amyloid deposits in Alzheimer's disease

Nobuyuki Okamura,¹ Shozo Furumoto,² Yoshihito Funaki,³ Takahiro Suemoto,⁴ Motohisa Kato,¹ Yoichi Ishikawa,³ Satoshi Ito,¹ Hiroyasu Akatsu,⁵ Takayuki Yamamoto,⁵ Tohru Sawada,⁴ Hiroyuki Arai,⁶ Yukitsuka Kudo² and Kazuhiko Yanai¹

¹Department of Pharmacology, Tohoku University Graduate School of Medicine, ²Tohoku University Biomedical Engineering Research Organization (TUBERO), ³Division of Radiopharmaceutical Chemistry, Cyclotron and Radioisotope Center, Tohoku University, ⁴Center for Asian Traditional Medicine, Department of Geriatrics and Gerontology, Tohoku University School of Medicine, Sendai, ⁴BF Research Institute, Osaka, and ⁵Fukushima Hospital, Toyohashi, Japan

Background: *In vivo* detection of amyloid deposits in the brain is potentially useful for early diagnosis of Alzheimer's disease (AD) and tracking the efficacy of anti-amyloid therapy.

Methods: To develop an amyloid-binding agent for positron emission tomography, we screened over 2600 compounds.

Results: We found benzoxazole derivatives as candidate compounds for *in vivo* amyloid imaging probes. One of these agents, 2-(2-[2-dimethylaminothiazol-5-yl]ethenyl)-6-(2-[fluoro]ethoxy)benzoxazole (BF-227), displays high binding affinity to A β fibrils. BF-227 binding increased linearly with increasing A β fibril formation. In temporal and hippocampal AD brain sections, BF-227 selectively bound to amyloid plaques. In contrast, no staining was evident in the cerebellum. Compared with the previously reported compound BF-168, ¹⁸F-labeled BF-227 displayed selective *in vivo* labeling of amyloid fibrils and rapid washout from white matter areas in an A β -injected rat model. An acute and subacute toxicity study of BF-227 indicated sufficient safety for clinical use as a positron emission tomography probe.

Conclusions: These findings suggest that BF-227 is feasible as an *in vivo* imaging probe of amyloid deposits in AD patients.

Keywords: Alzheimer's disease, amyloid, positron emission tomography, senile plaques.

Introduction

Progressive deposition of senile plaques (SP) and neurofibrillary tangles (NFT) is a critical event in the pathogenesis of Alzheimer's disease (AD). These lesions precede the presentation of clinical symptoms of dementia.¹ For early or presymptomatic diagnosis of AD, non-invasive detection of these lesions using positron emission tomography (PET) is a potentially

Accepted for publication 22 August 2007.

Correspondence: Dr Nobuyuki Okamura MD PhD, Department of Pharmacology, Tohoku University Graduate School of Medicine, 2-1 Seiryomachi, Aoba-ku, Sendai 980-8575, Japan.
Email: oka@mail.tains.tohoku.ac.jp

useful technique.² To achieve successful *in vivo* imaging using PET, sensitive and selective contrast agents to these lesions are needed. Congo red and thioflavin T have represented attractive lead compounds as developing amyloid-imaging agents, because these compounds selectively bind to β -pleated sheet structures and are commonly used for histochemical staining of SP. However, the permeability of these compounds through the blood-brain barrier (BBB) is extremely limited.³ The chemical structure must thus be optimized to provide appropriate lipophilicity without changing the binding properties to amyloid. Thioflavin T derivatives without any positive charge show high permeability of the BBB. One of these compounds, 6OH-BTA-1 (PIB), has been applied in a human PET study and enabled successful detection of early AD patients.⁴ Another compound, 2-(1-[6-(2-fluoroethyl)amino]-2-naphthyl]ethylidene) malononitrile (FDDNP), is extremely lipophilic and can easily penetrate the BBB, and specifically binds to both SP and NFT in AD brain sections.⁵ After i.v. injection of FDDNP, greater accumulation was observed in SP- and NFT-rich areas of the human brain.⁶ Although validation is still required as to whether retention of these agents in the neocortex truly reflects levels of amyloid deposition, such findings suggest the potential usefulness of this technique for early diagnosis of AD.

We have previously demonstrated a novel series of compounds including 6-(2-fluoroethoxy)-2-(2-[4-methylaminophenyl]ethenyl)benzoxazole (BF-168) and 2-(2-[4-methylaminophenyl]ethenyl)-5-fluoroben-

zoxazole (BF-145) as promising candidates for *in vivo* imaging probes of SP.⁷⁻⁹ These benzoxazole derivatives demonstrate high binding affinity for A β aggregates and high BBB permeability, suggesting potential utility as *in vivo* amyloid-binding agents. However, for the application of these compounds to clinical PET studies, the pharmacokinetic properties and pharmacological safety of these molecules requires improvement. This study describes the characterization of an optimized benzoxazole derivative, 2-(2-[2-dimethylaminothiazol-5-yl]ethenyl)-6-(2-[fluoro]ethoxy) benzoxazole (BF-227), as a candidate *in vivo* amyloid-imaging agent in humans.

Methods

Preparation of the compounds

BF-168, BF-227 (Fig. 1) and the precursor compounds for ¹⁸F-labeled agents were custom-synthesized by Tanabe R & D Service (Osaka, Japan). Synthesis of (¹⁸F)BF-168 was performed by reacting 2-(4-methylaminophenyl)-6-(2-tosyloxyethoxy) benzoxazole (Tanabe R & D Service) with (¹⁸F)KF and Kryptofix 222 (Merck, Darmstadt, Germany) in acetonitrile at 80°C for 20 min, as described previously.⁸ Radiosynthesis of (¹⁸F)BF-227 was performed using the same method. After subsequent high-performance liquid chromatography (HPLC) purification, ¹⁸F-labeled compounds were obtained (Fig. 1). Details of the radiosynthetic methods will be described elsewhere.

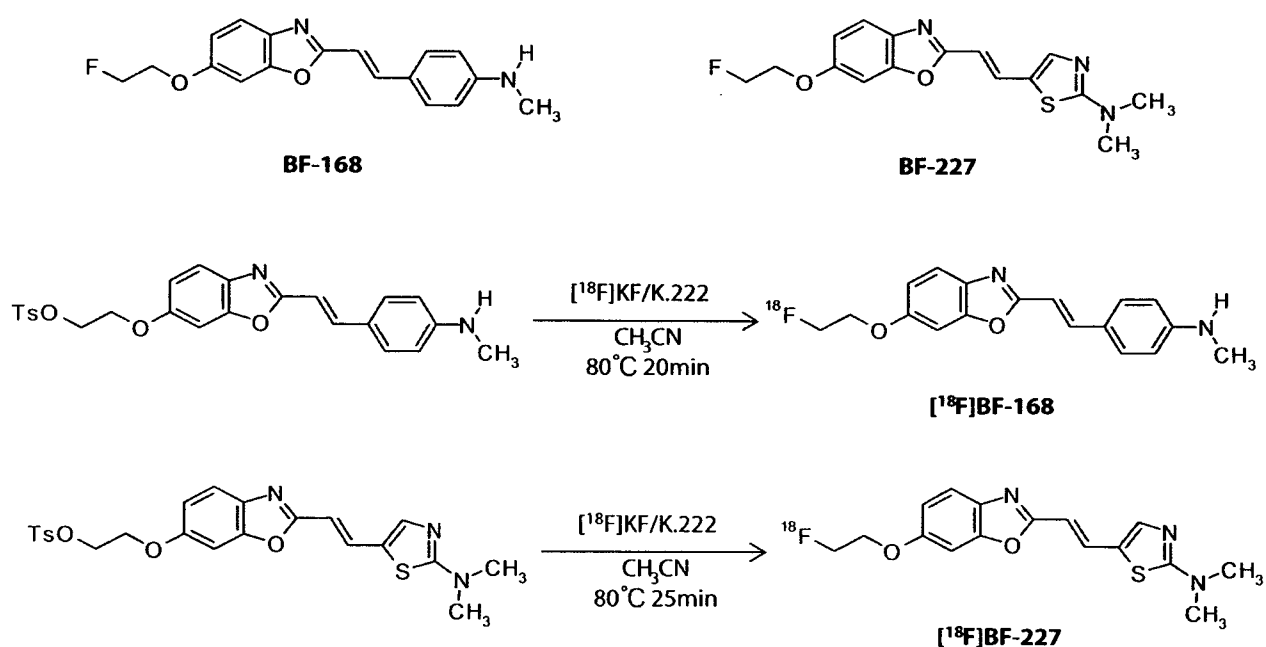


Figure 1 Chemical structures and radiosynthesis of BF-168 and BF-227.

In vitro binding assays

Binding affinities of the compounds for synthetic A β aggregates were examined as described previously.⁷ Briefly, solid-form A β 1–40 (Peptide Institute, Osaka, Japan) was dissolved in 10 mmol/L potassium phosphate buffer (pH 7.4) and incubated at 37°C for 72 h. The binding assay was performed by mixing aggregated A β 1–40 with the appropriate concentration of ¹⁸F-labeled BF-227, unlabeled BF-227 and dimethyl sulfoxide. After incubation for 10 min at room temperature, the binding mixture was filtered using a cell harvester (Model M-24; Brandel, Gaithersburg, MD, USA) and filters containing bound ¹⁸F ligand were counted using a γ -counter. The dissociation constant (K_d) of BF-227 was determined by Scatchard analysis.

Fluorometric analysis of BF-227 binding with A β fibrils was performed using the following method. A total of 20 μ mol/L of A β 1–40 or A β 1–42 (Peptide Institute) in 50 mmol/L of potassium phosphate buffer (pH 7.4) was incubated at 37°C on a Vibrax VXR shaker (IKA, Cincinnati, OH, USA) at 0.56 g. Before fluorometric analysis, A β solutions were sonicated for 3 min at 45 kHz using a VS-100III ultrasonic cleaner (Iuchi, Osaka, Japan). In fluorometry, A β 1–40 and A β 1–42 solutions at 0, 4, 8 and 24 h after the start of incubation were mixed with the same volume of BF-227 solution (5 μ mol/L final concentration). After determination of the optimal excitation wavelength for the mixture of BF-227 and A β , fluorescence spectra were measured using a Gemini XS microplate spectrofluorometer (Molecular Devices, Sunnyvale, CA, USA). In addition, fluorescence spectra for the mixture of 5 μ M BF-227 and different concentrations of A β 1–40 or A β 1–42 (0.15, 0.5, 1.5, 2.5, 5 and 10 μ mol/L final concentrations) at 96 h after incubation (fibrillar A β) were measured using the microplate spectrofluorometer. The same measurements were also performed using A β 1–40 and A β 1–42 with no incubation (non-fibrillar A β). All measurements were performed in triplicate.

Neuropathological staining

Postmortem brain tissues from an autopsy-confirmed AD case (69-year-old man) were obtained from Fukushima Hospital (Toyohashi, Japan). Experiments were performed under the regulations of the Ethics Committee of BF Research Institute. Serial sections (6- μ m thick) from paraffin-embedded blocks of temporal cortex and cerebellum were prepared in xylene and ethanol. Before staining, quenching of autofluorescence was performed as described previously. Quenched tissue sections were immersed in 100 μ mol/L of BF-227 solution for 10 min or 0.01% 1-bromo-2,5-bis(3-carboxy-4-hydroxystyryl)benzene (BSB) solution containing 50% ethanol for 30 min. Sections stained with BF-227 were then dipped briefly

into water and rinsed in phosphate-buffered saline (PBS) for 60 min before coverslipping with Fluor Save Reagent (Calbiochem, La Jolla, CA, USA), and examined using an Eclipse E800 microscope (Nikon, Tokyo, Japan) equipped with a V-2A filter set (excitation 380–420 nm, dichroic mirror 430 nm, longpass filter 450 nm). Sections stained with BSB were dipped briefly in tap water and then in 50% ethanol, then washed in PBS for 60 min before coverslipping, followed by fluorescent microscopy using a BV-2A filter set (excitation 400–440 nm, dichroic mirror 455 nm, longpass filter 470 nm). In addition, adjacent sections were immunostained using monoclonal antibody (mAb) against A β (6F/3D; Dako A/S, Glostrup, Denmark). After pretreatment with 90% formic acid for 5 min, sections were immersed in blocking solution for 30 min and then incubated for 60 min at 37°C with 6F/3D at a dilution of 1:50. Following incubation, sections were processed by the avidin–biotin method using a Pathostain ABC-POD(M) Kit (Wako, Osaka, Japan) and diaminobenzidine tetrahydrochloride. Fluorescence intensity of three different brain slices stained with BF-227 was analyzed by defining regions of interest (ROI) and measuring the intensity of fluorescence within gray and white matter using Lumina Vision software (Mitani, Fukui, Japan). Ratios of gray matter ROI to white matter ROI were calculated as an indicator of stainability and statistical comparisons were performed using ANOVA and Scheffe post-hoc tests.

Labeling of amyloid deposits in A β -injected rat model

A β 1–40 (Peptide Institute) was dissolved at 500 μ mol/L in 50 mmol/L potassium phosphate buffer and incubated at 37°C for 4 days. An A β -injected rat model was created as described previously.¹⁰ Briefly, Wistar rats (male, 200–250 g, SLC, Shizuoka, Japan) were injected with A β peptides unilaterally and potassium phosphate buffer contralaterally into each amygdala using a stereotaxic instrument (Model 5000, David Kopf, Tujunga, CA, USA). Injection coordinates measured from the bregma and skull surface (anteroposterior, –3.0 mm; mediolateral, \pm 5.0 mm; dorsoventral, –8.8 mm) were determined based on a stereotaxic atlas.¹¹ A volume of 1.0 μ L was administered over 2 min using a microsyringe and glass cannula (tip diameter, 170–250 μ m). At 3 days after injection of A β and vehicle, (¹⁸F)BF-168 (72.8 MBq) or (¹⁸F)BF-227 (58.9 MBq) were administered into the femoral vein of anesthetized rats. Rats were killed by decapitation at 180 min postinjection and the brains were removed and frozen. An OTF cryostat (Bright Instruments, Huntingdon, UK) was used to cut 30- μ m thick frozen sections, which were then dried and exposed to a BAS-III imaging plate for 18 h. Autoradiographic images were obtained using a BAS2000 scanner system

(Fuji Film, Tokyo, Japan). After autoradiographic examination, the same sections were stained with thioflavin-S to confirm the presence of amyloid plaques.

Toxicity study in mice

A non-GLP (good laboratory practice) toxicity study was performed using female and male ICR mice (weight, 22–32 g). The Ethics Committee of BF Research Institute approved the protocol for these experiments. Animals were kept in a temperature-controlled environment (21.2–23.5°C) with a 12-h light–dark cycle and ad libitum access to food and water. In the acute toxicity study, animals were divided into one control group and three treated groups, with 10 animals (five males, five females) in each group. The control group received injection of vehicle alone, while each treated group received i.v. injection of BF-227 solution in doses of 0.1, 1 or 10 mg/kg. Animals were observed for 8 days after administration to identify any changes in general behavior or bodyweight. In the subacute toxicity study, animals were divided into one control group and two treated groups (2.5 and 25 µg/kg), with 10 animals (five females, five males) in each group. The control group received injection of vehicle alone and each treated group received i.v. injection of BF-227 solution for 14 days (once daily). Animals were weighed at 3, 7, 9 and 14 days after administration. At the end of the experiment, animals were sacrificed and examined at autopsy. Selected organs (brain, heart, liver, lung and kidney) were removed, weighed and examined microscopically by a pathologist.

Results

Binding characteristics of BF-227 for Aβ fibrils

In vitro binding assay indicated that BF-227 shows high binding affinity for Aβ fibrils. K_d for Aβ1–40 fibrils was 1.0 ± 1.4 nmol/L, comparable to previously reported levels for amyloid imaging agents¹² (Fig. 2). Binding ability of BF-227 to Aβ was also examined by fluorometric analysis, as BF-227 is highly fluorescent. In the mixture of BF-227 and Aβ peptides, fluorescence intensity of BF-227 increased as Aβ1–40 (Fig. 3a) and Aβ1–42 (data not shown) incubation time advanced. BF-227 fluorescence also increased in a linear manner with increasing concentrations of fibrillar Aβ1–42 (Fig. 3b) or Aβ1–40 (data not shown), but did not increase in mixture with non-fibrillar Aβ. These results suggest that degree of BF-227 binding reflects the amount of Aβ fibril formation.

Neuropathological staining in AD brain sections

Neuropathological examination using BF-227 indicated that amyloid plaques were clearly stained with BF-227

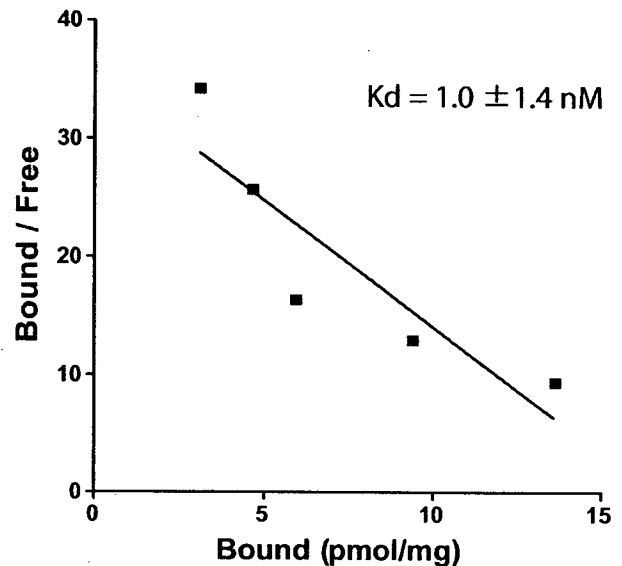


Figure 2 Scatchard plots of (¹⁸F)BF-227 binding to synthetic Aβ fibrils.

in AD brain sections (Fig. 4a). In particular, cored plaques stained brightly with this compound. This staining pattern correlated well with Aβ immunostaining in adjacent sections (Fig. 4b). BF-227 staining was further compared to staining using BSB, a Congo red derivative. In contrast to clear staining of SP and NFT with BSB (Fig. 4c), BF-227 primarily stained SP, with faint staining of NFT. Preferential binding of BF-227 to SP rather than NFT represents a similar characteristic to the previously reported compound BF-145. BF-227 staining was subsequently performed in three different regions (temporal lobe, hippocampus and cerebellum) of an AD brain. In temporal (Fig. 5a) and hippocampal (Fig. 5b) sections, cored plaques stained brightly with BF-227. In contrast, no staining was evident in the cerebellum (Fig. 5c). Fluorometric measurement of these brain sections indicated that overall level of stainability in the cerebellum differed significantly from that in the temporal cortex and hippocampus (Fig. 5d), suggesting the binding specificity of this compound to AD pathology.

Intravenous administration of ¹⁸F-labeled agents in Aβ-injected rat model

In vivo binding ability of (¹⁸F)BF-168 and (¹⁸F)BF-227 to Aβ fibrils was further evaluated by the autoradiographic experiment in the Aβ-injected rat model. In an image of the brain section at 180 min postinjection of ¹⁸F-labeled agents (Fig. 6), Aβ aggregates were clearly labeled with both agents, suggesting the usefulness of these agents as *in vivo* amyloid-imaging probes. However, non-specific

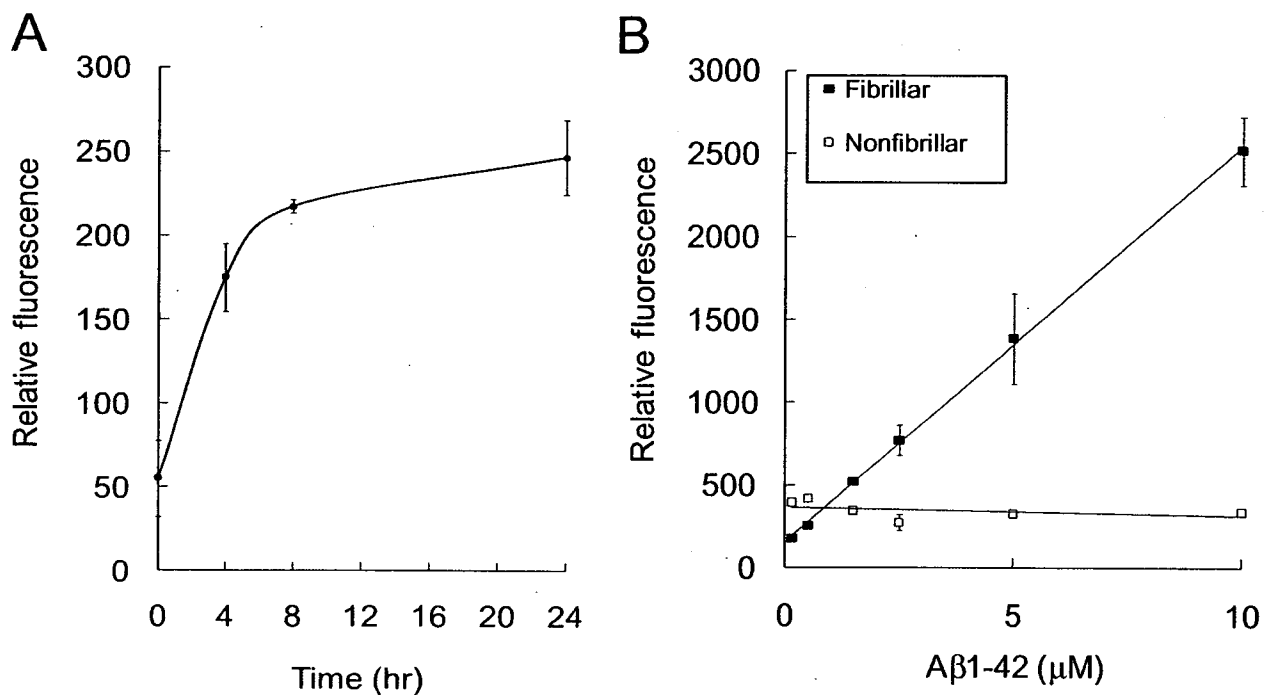


Figure 3 *In vitro* binding of BF-227 with Aβ peptides. Fluorescence intensity of BF-227 increased with Aβ incubation time (A). BF-227 fluorescence also increased linearly with concentrations of fibrillar Aβ, but did not increase in mixture with non-fibrillar Aβ (B).

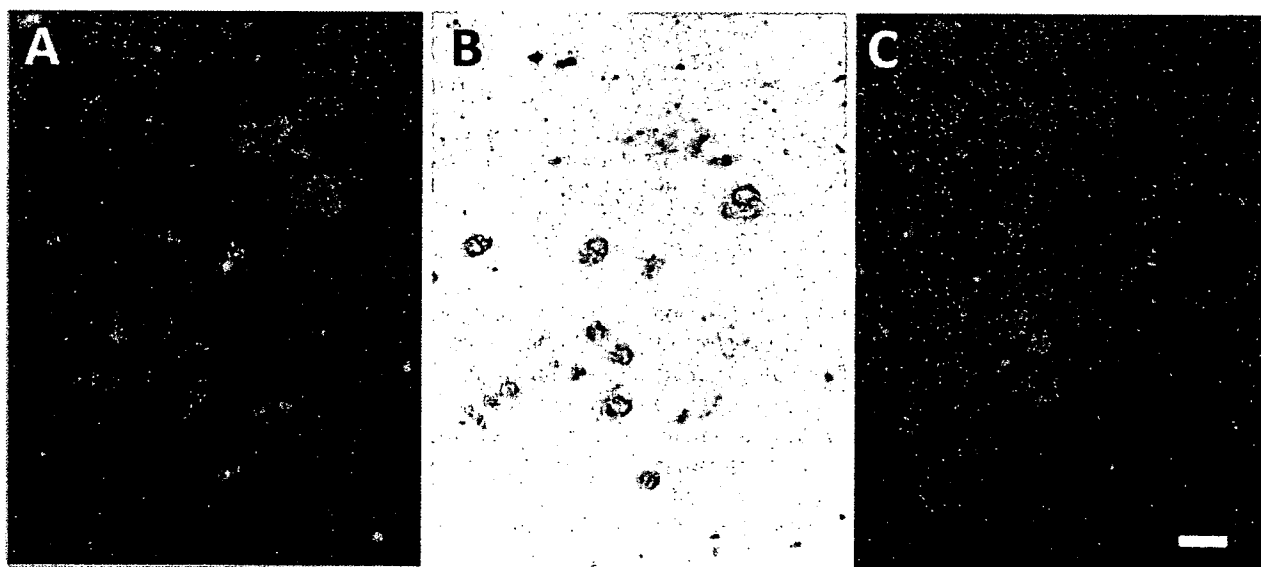


Figure 4 Neuropathological staining of Alzheimer's disease (AD) temporal brain sections by BF-227. Senile plaques are clearly stained by BF-227 (A). This staining correlates well with Aβ immunostaining in adjacent sections (B). BSB stains both senile plaques and neurofibrillary tangles (C). Bar, 200 μm.

retention of (¹⁸F)BF-227 in the white matter was much less than that of (¹⁸F)BF-168. This resulted in better hot spot-to-background contrast for (¹⁸F)BF-227 (Fig. 6b) compared to (¹⁸F)BF-168 (Fig. 6a).

Toxicity study of BF-227

In the acute toxicity study, i.v. administration of BF-227 in doses 0.1–10 mg/kg did not produce any significant

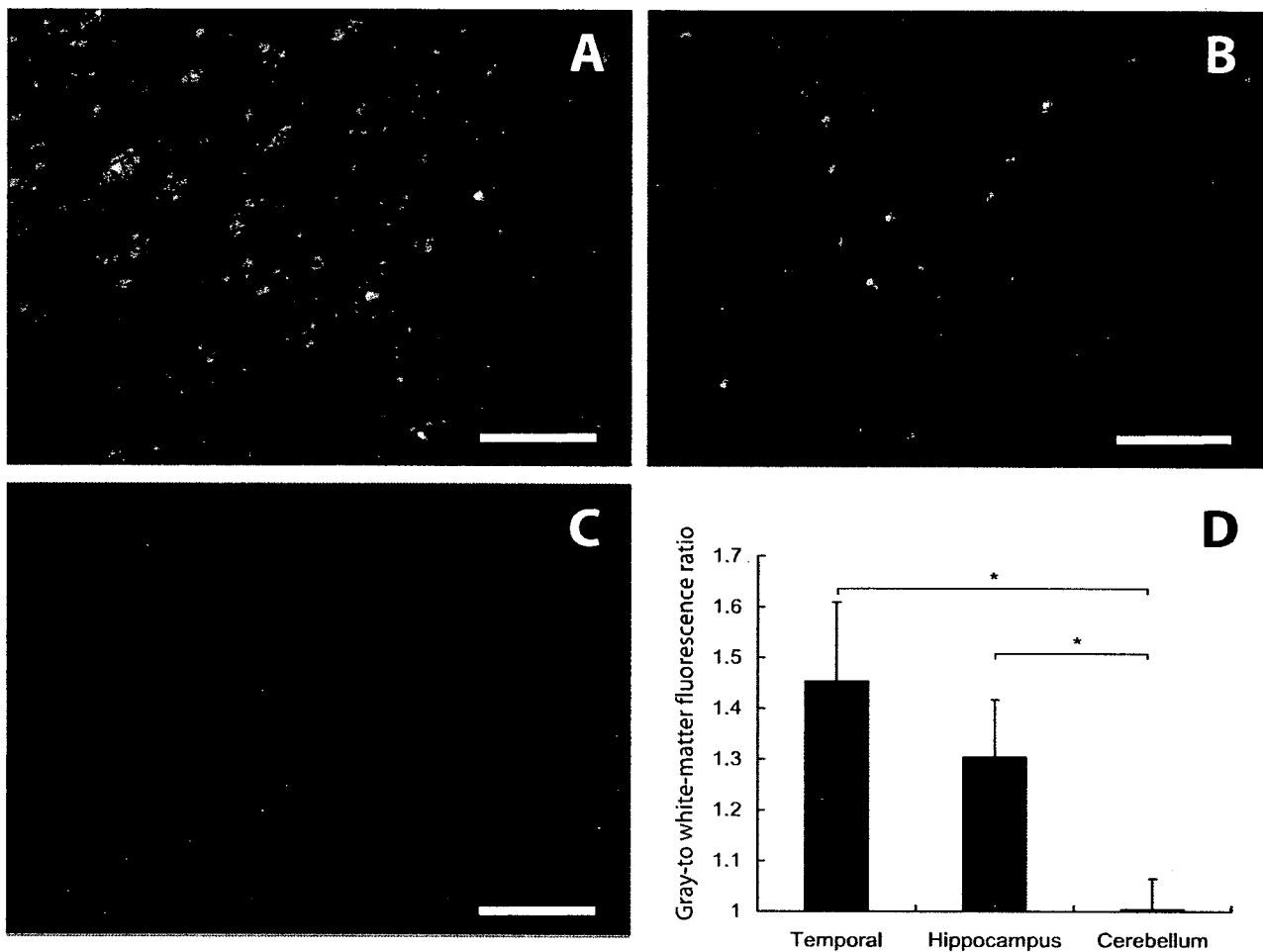


Figure 5 BF-227 staining in the temporal cortex (A), hippocampus (B) and cerebellum (C) of AD brain. In temporal and hippocampal brain sections, large numbers of amyloid plaques stained with BF-227. In contrast, no apparent staining was observed in the cerebellum. The stainability of BF-227 in the temporal cortex and hippocampus differed significantly from that in the cerebellum (D). * $P < 0.05$, one-way ANOVA followed by Scheffe's test.

changes in general behavior or bodyweight in male or female mice. During the 8 days of the experiment, no deaths occurred in any of the groups. This indicates that the dose for 50% lethality (LD_{50}) of i.v. administered BF-227 is higher than 10 mg/kg for male and female mice. In the subacute toxicity study, i.v. administration of BF-227 in tested doses did not produce any significant changes in general behavior or bodyweight in male or female mice. No significant differences in organ weight were observed between control and BF-227-administered groups. After the 14-day post-treatment period, mice did not show any microscopic alterations on pathological examination.

Discussion

Several research groups have worked to develop amyloid-imaging agents for use with PET. PIB is cur-

rently the most successful of these agents, showing high binding affinity for $A\beta$ fibrils and fast clearance from normal brain tissue.¹³ In the clinical trial, PIB-PET distinctly differentiated AD patients from normal individuals.⁴ Other amyloid-imaging agents, such as SB-13,¹⁴ IMPY¹⁵ and benzofuran derivatives,¹⁶ have also been explored for use as PET and single-photon emission computed tomography (SPECT) imaging probes. These agents display high binding affinity to $A\beta$ fibrils. The key chemical structure common to these imaging agents is an aminophenyl group, which is considered essential for binding to the β -pleated sheet structure of $A\beta$ fibrils. The present study, however, demonstrated that BF-227, a derivative of BF-168 with an aminothiazol group in place of the aminophenyl group, also binds strongly to amyloid- β fibrils. Furthermore, an autoradiographic study comparing BF-227 to BF-168 suggested that the aminothiazol group might contribute in a large way to

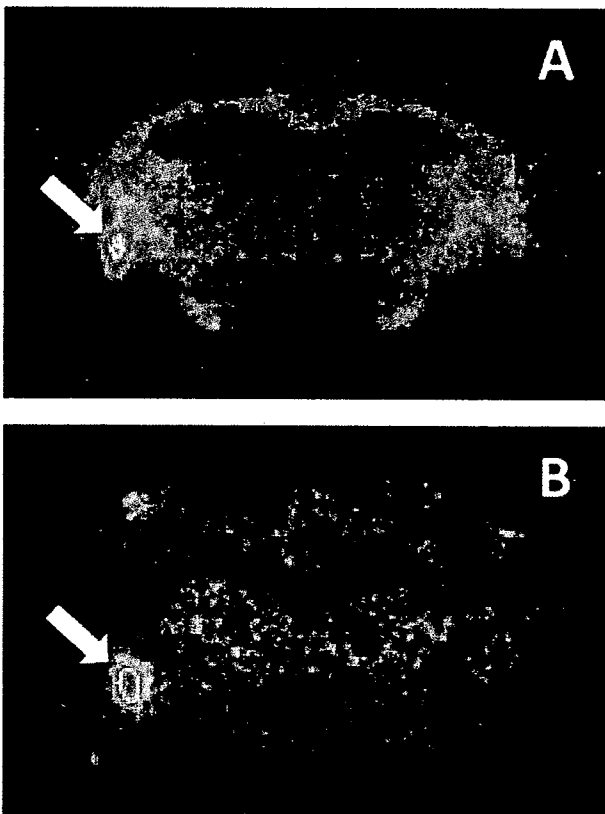


Figure 6 *In vivo* labeling of A β fibrils in brain sections from the A β -injected rat model with (^{18}F)BF-168 (A) and (^{18}F)BF-227 (B). Arrows indicate sites of A β injection.

decreased non-specific retention in normal brain tissue, particularly in white matter. This possibility should be examined in further studies, as this finding would be helpful in the design or modification of further series of amyloid-imaging agents.

Findings from the *in vitro* binding experiment indicated that the amount of BF-227 binding is proportional to the concentration of A β fibrils. Neuropathological findings also indicated that BF-227 preferentially binds to lesions containing dense A β fibrils. Densities of neuritic plaques are higher in the temporal, parietal and occipital lobes, moderate in the limbic lobe and lowest in the cerebellum.¹⁷ Our results for BF-227 stainability in different brain regions were consistent with this neuropathological pattern of A β deposition in AD patients. Brains from patients with AD are characterized by an anatomically widespread process of amyloid deposition. Presence of neuritic or cored plaques is considered the best indication of the presence of the disease process underlying AD.¹⁸ Quantitative measurement of A β fibril formation using BF-227 will thus allow discrimination of the disease process from normal aging processes. SP in the cerebellum are predominantly of the non-fibrillar type. The lack of obvious staining by BF-227 in the

cerebellum thus suggests the binding preference of this compound to fibrillar A β .

The present study demonstrated high binding affinity of BF-227 to fibrillar A β and preferential binding to SP in AD brain sections. *i.v.* administration of this compound into an A β -injected rat model demonstrated selective binding to amyloid fibrils in the brain and faster clearance from white matter than BF-168. The toxicity study indicated that BF-227 is safe for clinical use as a PET probe, with a very wide margin between the lethal dose of BF-227 (>10 mg/kg) and clinical dose in human PET studies (<100 ng/kg). Considering all these findings together, BF-227 appears applicable for use as an *in vivo* amyloid-imaging agent. We are currently engaging in a clinical PET trial using ^{11}C -labeled BF-227 in AD patients.¹⁹ This trial will elucidate the clinical utility of BF-227 in humans.

Acknowledgments

This study was partially supported by the Novartis Foundation for Gerontological Research, the Special Coordination Funds for Promoting Science and Technology, the Program for the Promotion of Fundamental Studies in Health Science by the National Institute of Biomedical Innovation, the Industrial Technology Research Grant Program from the New Energy and Industrial Technology Development Organization (NEDO) of Japan, Health and Labor Sciences Research Grants for Translational Research from the Japanese Ministry of Health, Labor and Welfare, a JST grant on research and education in molecular imaging, and an AstraZeneca Research Grant.

References

- 1 Price JL, Morris JC. Tangles and plaques in nondemented aging and "preclinical" Alzheimer's disease. *Ann Neurol* 1999; 45: 358–368.
- 2 Nordberg A. PET imaging of amyloid in Alzheimer's disease. *Lancet Neurol* 2004; 3: 519–527.
- 3 Klunk WE, Wang Y, Huang GF, Debnath ML, Holt DP, Mathis CA. Uncharged thioflavin-T derivatives bind to amyloid-beta protein with high affinity and readily enter the brain. *Life Sci* 2001; 69: 1471–1484.
- 4 Klunk WE, Engler H, Nordberg A *et al.* Imaging brain amyloid in Alzheimer's disease with Pittsburgh Compound-B. *Ann Neurol* 2004; 55: 306–319.
- 5 Agdeppa ED, Kepe V, Liu J *et al.* Binding characteristics of radiofluorinated 6-dialkylamino-2-naphthylethylidene derivatives as positron emission tomography imaging probes for beta-amyloid plaques in Alzheimer's disease. *J Neurosci* 2001; 21: RC189.
- 6 Small GW, Kepe V, Ercoli LM *et al.* PET of brain amyloid and tau in mild cognitive impairment. *N Eng J Med* 2006; 355: 2652–2663.
- 7 Okamura N, Suemoto T, Shimadzu H *et al.* Styrylbenzoxazole derivatives for *in vivo* imaging of amyloid plaques in the brain. *J Neurosci* 2004; 24: 2535–2541.

- 8 Shimadzu H, Suemoto T, Suzuki M *et al.* Novel probes for imaging amyloid- β : F-18 and C-11 labeling of 2-(4-aminostyryl) benzoxazole derivatives. *J Label Compd Radiopharm* 2004; **47**: 181–190.
- 9 Okamura N, Suemoto T, Shiomitsu T *et al.* A novel imaging probe for in vivo detection of neuritic and diffuse amyloid plaques in the brain. *J Mol Neurosci* 2004; **24**: 247–255.
- 10 Suemoto T, Okamura N, Shiomitsu T *et al.* In vivo labeling of amyloid with BF-108. *Neurosci Res* 2004; **48**: 65–74.
- 11 Paxinos G, Watson C. *The Rat Brain in Stereotaxic Coordinates*. San Diego, CA: Academic Press, 1998.
- 12 Mathis CA, Klunk WE. Imaging β -amyloid plaques and neurofibrillary tangles in the aging human brain. *Curr Pharm Design* 2004; **10**: 1469–1492.
- 13 Mathis CA, Wang Y, Holt DP, Huang GF, Debnath ML, Klunk WE. Synthesis and evaluation of ^{11}C -labeled 6-substituted 2-arylbenzothiazoles as amyloid imaging agents. *J Med Chem* 2003; **46**: 2740–2754.
- 14 Verhoeff NP, Wilson AA, Takeshita S *et al.* In-vivo imaging of Alzheimer disease beta-amyloid with [^{11}C]SB-13 PET. *Am J Geriatr Psychiatry* 2004; **12**: 584–595.
- 15 Kung MP, Hou C, Zhuang ZP *et al.* Characterization of IMPY as a potential imaging agent for β -amyloid plaques in double transgenic PSAPP mice. *Eur J Nucl Med Mol Imaging* 2004; **31**: 1136–1145.
- 16 Ono M, Kawashima H, Nonaka A *et al.* Novel benzofuran derivatives for PET imaging of β -amyloid plaques in Alzheimer's disease brain. *J Med Chem* 2006; **49**: 2725–2730.
- 17 Arnold SE, Hyman BT, Flory J, Damasio AR, Van Hoesen GW. The topographical and neuroanatomical distribution of neurofibrillary tangles and neuritic plaques in the cerebral cortex of patients with Alzheimer's disease. *Cereb Cortex* 1991; **1**: 103–116.
- 18 Price JL. Diagnostic criteria for Alzheimer's disease. *Neurobiol Aging* 1997; **18**: S67–S70.
- 19 Kudo Y, Okamura N, Furumoto S *et al.* 2-[2-(2-dimethylaminothiazol-5-yl) ethenyl] -6-[2-(fluoro) ethoxy]benzoxazole: a novel PET imaging agent for in vivo detection of dense amyloid plaques in Alzheimer's disease patients. *J Nucl Med* 2007; **48**: 553–561.

Altered Expression of COX-2 in Subdivisions of the Hippocampus during Aging and in Alzheimer's Disease: The Hisayama Study

Kouhei Fujimi^{a,d} Kazuhito Noda^a Kensuke Sasaki^a Yoshinobu Wakisaka^{a,b}
Yumihiko Tanizaki^b Mitsuo Iida^b Yutaka Kiyohara^c Shigenobu Kanba^d
Toru Iwaki^a

^aDepartment of Neuropathology, Neurological Institute, Departments of ^bMedicine and Clinical Sciences, ^cEnvironmental Medicine, and ^dPsychiatry, Graduate School of Medical Sciences, Kyushu University, Fukuoka, Japan

Key Words

Cyclooxygenase · Alzheimer's disease · Hippocampus

Abstract

Background: It has been reported that nonsteroidal anti-inflammatory drugs may delay the onset of Alzheimer's disease (AD). Since nonsteroidal anti-inflammatory drugs inhibit cyclooxygenase (COX), COX-2, an inducible form of COX, may be involved in the pathology of AD in association with the arachidonic acid cascade. In addition, it has been suggested that alterations in the balance of polyunsaturated fatty acids are associated with brain dysfunctions such as neurodegenerative pathologies of the aging brain. **Method:** To explore COX-2 expression in the hippocampus, we analyzed 45 consecutive autopsy subjects without dementia and 25 AD patients derived from the town of Hisayama, Japan. **Results:** The neuronal expression of COX-2 in the CA3 subdivision of the hippocampus, subiculum, entorhinal cortex and transentorhinal cortex were consistently observed in both nondemented and AD brains, and COX-2 immunoreactivity correlated with age in nondemented brains. In AD patients, neurons of CA1 exhibited increased COX-2 immunoreactivity which correlated with the severity of AD pathology. This correlation was not apparent in nondemented subjects. **Conclusion:** These results suggest that COX-2 expression may be

differentially regulated among subdivisions of the hippocampus and that elevated COX-2 expression in the CA1 of AD brains may be associated with AD pathology and thus cognitive dysfunction.

Copyright © 2007 S. Karger AG, Basel

Introduction

Many epidemiological studies suggest that the use of nonsteroidal anti-inflammatory drugs delays or slows the clinical expression of Alzheimer's disease (AD) [1, 2]. The mechanism by which these drugs might affect pathophysiological processes relevant to AD remains unclear. Most nonsteroidal anti-inflammatory drugs have an inhibitory effect on cyclooxygenase (COX), an enzyme involved in the metabolism of arachidonic acid into prostanoids. There are two major known COX isoforms, the constitutively expressed COX-1 and the mitogen-inducible COX-2 [3]. While COX-1 is mainly expressed in microglia and some neuronal cells throughout the brain, COX-2 is expressed in neurons [4, 5]. It has been suggested that alterations in the balance of polyunsaturated fatty acids, including arachidonic acid and its metabolites, in the central nervous system are associated with brain dysfunction, such as in neurodegenerative pathologies of the aging

brain [6]. Following on these epidemiological reports, several histological analyses of COX-2 expression in AD brains have been conducted [4, 7–11], but have produced conflicting results. Several studies reported increased neuronal COX-2 immunoreactivity compared to control brain tissues [5, 7]. However, in other studies, in which COX-2 expression was related to specific hallmarks of the disease, such as clinical dementia rating and Braak stage of disease, the number of COX-2-positive neurons decreased with the severity of dementia, and in the end-stage AD, COX-2-positive neurons were significantly fewer than in nondemented controls [4, 11].

Although many studies have been conducted concerning COX-2 expression not only in AD brains, but also in Parkinson disease model mice brains [12], amyotrophic lateral sclerosis brains [13] and schizophrenia brains [14], the histological analyses concerning COX-2 expression in nondemented brains are few. Now that we know that COX-2 expresses constitutively in the brain even under normal conditions [15], it is important to explore the normal COX-2 expression pattern in the brain. Without this basic knowledge, it is difficult to interpret the conflicting results of COX-2 expression in AD brains.

In this study, we investigated the neuronal expression of COX-2 in some subdivisions of hippocampi of consecutive autopsy cases without dementia. In addition, we quantified senile plaque (SP) and neurofibrillary tangle (NFT) density to assess the influence of AD pathology on neuronal COX-2 expression, and explored any differences in the pattern of COX-2 expression in these regions between nondemented subjects and AD patients.

Materials and Methods

Subjects

To minimize the selection bias of the nondemented subjects, we collected the nondemented subjects from the series of consecutive autopsy cases in the Hisayama study. The Hisayama study is a prospective population-based study in the suburban community of Hisayama, which is adjacent to the metropolitan area of Fukuoka on Kyushu Island, Japan, and it started in 1961 [16–19]. We have carried out autopsies on most deceased subjects from this region in order to confirm the cause of death and to examine brain pathology. This paradigm has allowed a reliable recruitment of nondemented subjects in which to analyze the neuronal expression of COX-2. The diagnosis of dementia was based on the guidelines of the Diagnostic and Statistical Manual of Mental Disorders, Revised Third Edition [20]. For the clinical diagnosis of AD, we used the guidelines of the National Institute of Neurological and Communicative Disorders and Stroke and the Alzheimer's Disease and Related Disorders Association [21].

From October 1, 1998, to March 31, 2001, 148 Hisayama residents of varying initial ages died, 105 of whom (70.5%) underwent a postmortem examination. Consent to autopsy was unobtainable from 29.5% of the residents due to refusal, mainly on religious grounds. Of those 105 cases, 103 subjects received autopsies at the Departments of Pathophysiological and Experimental Pathology, Anatomic Pathology and Neuropathology of Kyushu University. In order to collect consecutive autopsy cases without dementia, we excluded 58 cases that were clinically diagnosed as exhibiting dementia or had some disease or condition that might influence the expression of COX-2 in the brain, such as severe chronic hepatic failure, autoimmune disease, disseminated intravascular coagulation, systemic inflammatory response syndrome, acute brain infarction, brain infection or a brain tumor. In total, 45 cases were analyzed in study A as nondemented subjects. In study B, in order to compare the nondemented subjects with AD patients, we examined all of the nondemented subjects aged 76 years or more at death of the nondemented subjects of study A and age- and sex-matched AD autopsy cases derived from Hisayama Town as the comparison group. In total, 25 nondemented subjects and 25 AD patients were analyzed in study B. We examined only cases aged 76 or more because there were few AD patients younger than 75 in the Hisayama study.

Neuropathological Assessment

Brains were weighed, evaluated for gross detectable lesions, abnormalities of the blood vessels and were fixed with 10% buffered formalin for at least 2 weeks. Brain specimens were taken following the Consortium to Establish a Registry for Alzheimer's Disease (CERAD) guidelines and the consensus guidelines for dementia with Lewy bodies [22, 23]. Thus, the specimens in each case included the middle frontal gyrus, superior and middle temporal gyri, inferior parietal lobule, anterior cingulate gyrus, hippocampus with entorhinal cortex and transentorhinal cortex (at the level of the lateral geniculate body), calcarine cortex, basal ganglia, thalamus, substantia nigra, locus coeruleus and dorsal vagal nucleus. Samples were embedded in paraffin and cut into sections which were routinely stained using hematoxylin-eosin and a modified Bielschowsky method. Each case was also immunostained with anti-tau (polyclonal, rabbit, 1:200, Dako, Denmark), anti-ubiquitin (polyclonal, rabbit, 1:100, Dako) and anti- α -synuclein (LB509: monoclonal, mouse, 1:100, provided by Dr. Iwatubo) [24]. Immunolabeling was detected using a standard indirect immunoperoxidase method and visualized with diaminobenzidine (Dojindo, Japan). The sections were lightly counterstained with hematoxylin.

Assessment of AD Pathology

The presence of SPs was estimated by a modified Bielschowsky method. NFT presence was assessed by tau immunohistochemistry. In each case, the frequency of SPs and NFTs were evaluated and converted to a plaque score according to CERAD criteria and Braak stage for tau pathology as established by Braak and Braak [22, 25]. The CERAD score and Braak stage were combined to estimate the likelihood of AD according to the NIA-RI criteria [26]. A diagnosis of AD was made when 'definite AD' as defined by the CERAD criteria and/or a 'high-likelihood' as defined by the NIA-RI criteria were found.

In addition, SP and NFT levels in the CA1 subdivision of the hippocampus were assessed. The semiquantitative density of SPs in

CA1 was determined as being either none, sparse, moderate, or frequent, according to the guidelines established by CERAD. NFTs in CA1 were counted in 100× fields at each of three locations and the average was expressed as the NFT number per 100× field.

Immunohistochemistry and Assessment of COX-2

Immunohistochemistry was performed on 7-μm paraffin-embedded sections encompassing the hippocampus, entorhinal cortex and transentorhinal cortex (at the level of the lateral geniculate body). Sections were deparaffinized in xylene, hydrated in an ascending ethanol series and incubated in 0.3% hydrogen peroxide in absolute methanol for 30 min at room temperature to inhibit endogenous peroxidase activity. After rinsing with tap water, the sections were pretreated with 90% formic acid for 10 min and autoclaved at 121°C for 10 min in 0.01 M citrate buffer, pH 6.0, in order to enhance immunoreactivity. After washing with Tris-HCl buffer (50 mM Tris-HCl, pH 7.6), an anti-human COX-2 (polyclonal, rabbit, 1:100, Cayman Chemical Co.) was applied. The slides were incubated overnight at 4°C and then sequentially incubated for 1 h with a biotinylated secondary antibody diluted 1:200, and a peroxidase-conjugated streptavidin-biotin complex diluted 1:100 sequentially (Amersham, UK). The colored reaction product was developed with 3,3'-diaminobenzidine tetrahydrochloride solution. The sections were then lightly counterstained with hematoxylin.

For analysis of neuronal COX-2 immunoreactivity, the mean gray values of a random-selected 5 neurons and 5 neuropil backgrounds were quantified using ImageJ 1.36b (National Institute of Health, USA) and the average was calculated. Then, we converted the mean gray value into a density using the following equation; uncalibrated density = $\log_{10}(255/\text{the mean gray value})$. Finally, we calculated the index that the neuronal density was divided by the neuropil background density, and we considered this index as the neuronal immunostaining density of COX-2. This index was calculated in CA1, CA3, subiculum entorhinal cortex and transentorhinal cortex.

The investigator was blind to the diagnosis of each case until analysis was completed and values were assigned to each specimen.

Statistical Methods

The quantitative data obtained were compared between the groups by Mann-Whitney's U test. Statistical significance was defined as $p < 0.05$. Correlation analysis was done using the Pearson parametric and Spearman nonparametric methods.

Results

Study A

Clinico-Neuropathological Information of Nondemented Subjects

The number of the nondemented subjects was 45 (M/F: 28/17). The ages at death were between 40 and 95 years and mean age at death was 76.4 ± 12.1 years. The brain weight was $1,264.0 \pm 166.8$ g (mean \pm SD) and postmortem time was 13.1 ± 9.3 h (mean \pm SD).

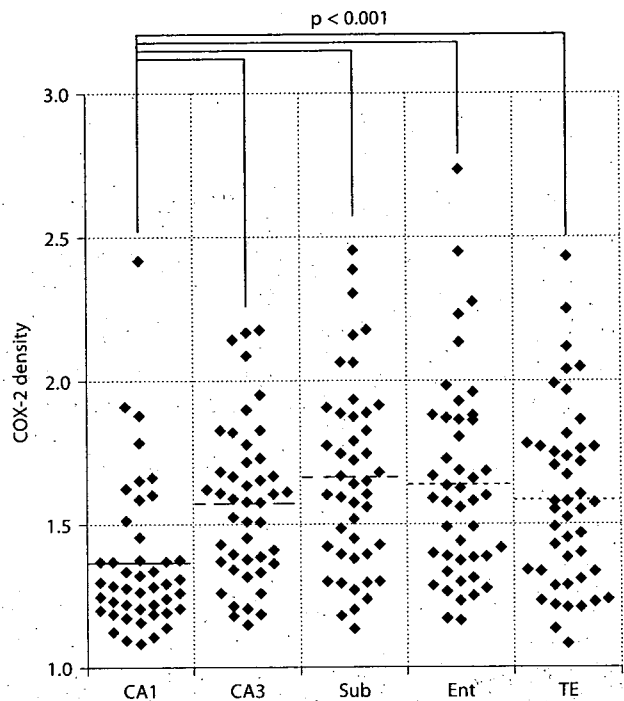


Fig. 1. Degrees of COX-2 immunoreactivity in different hippocampal subdivisions of nondemented subjects. Immunoreactivity is weak in CA1 as compared to all of the other fields examined with high statistical significance (Mann-Whitney U test, $p < 0.001$). Bars represent the mean density of neurons in each area. Sub = Subiculum; Ent = entorhinal cortex; TE = transentorhinal cortex.

COX-2 Immunoreactivity in the Hippocampus

The degree of COX-2 immunoreactivity in different hippocampal subdivisions of nondemented subjects is shown in figure 1. In nondemented subjects, the neuronal COX-2 immunoreactivity in CA3, subiculum, entorhinal cortex and transentorhinal cortex were strong (fig. 2a, d). On the other hand, the neuronal COX-2 immunoreactivity in CA1 was weak (fig. 2a, c) compared to all of the other fields examined, with high statistical significance (Mann-Whitney U test, $p < 0.001$). From these results, the constitutive expressions of COX-2 in CA3, subiculum, entorhinal cortex and transentorhinal cortex were thought to be strong, while weak in CA1.

COX-2 Immunoreactivity Correlates with Age in Nondemented Subjects

The correlation between neuronal COX-2 immunoreactivity and age is shown in figure 3. In the CA3 subdivi-

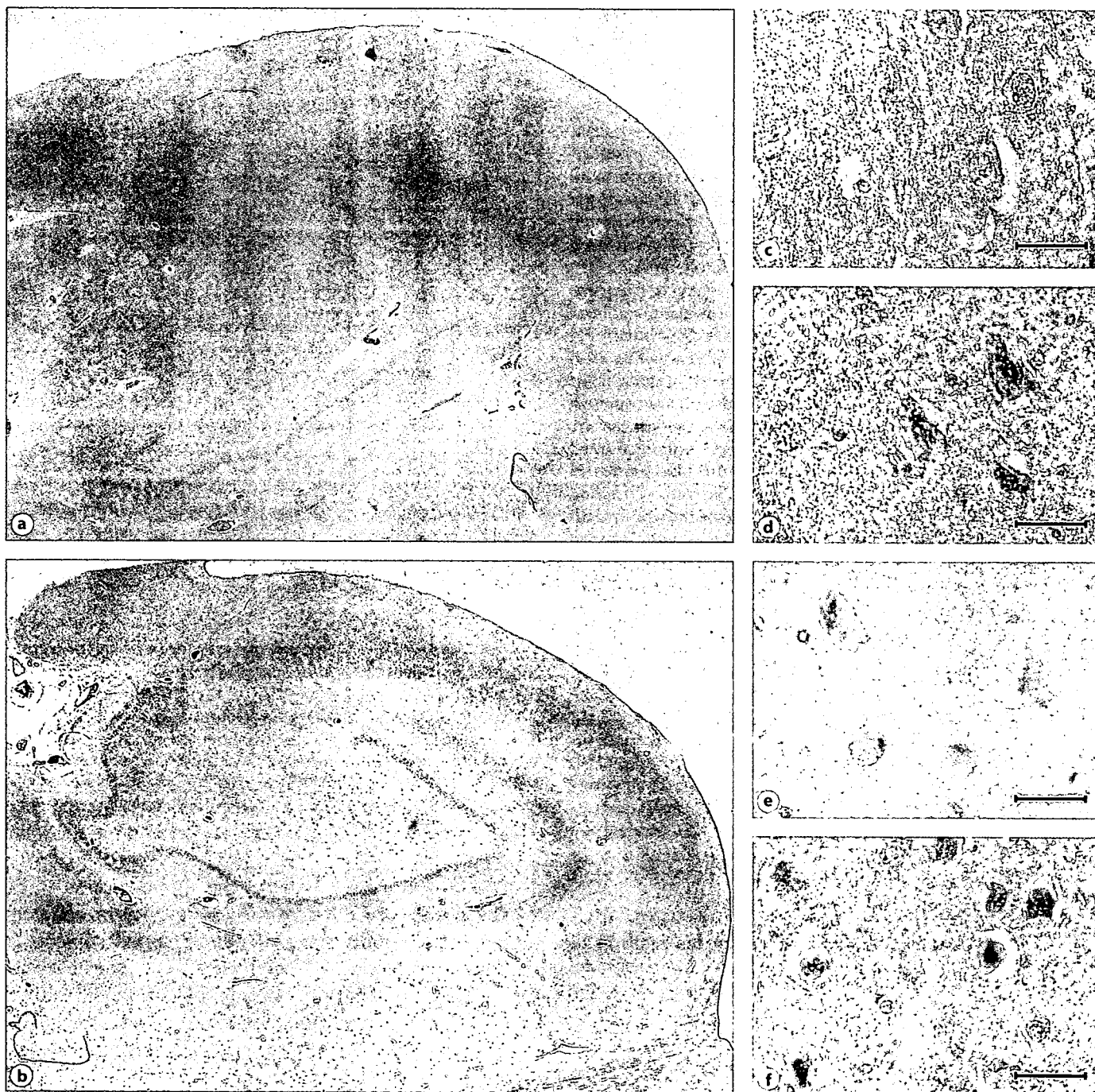


Fig. 2. COX-2 immunostaining in pyramidal neurons of the hippocampal formation in the brains of nondemented subjects (**a, c, d**) and in AD patients (**b, e, f**). **a, b** CA1-CA4 fields under low power. **c, e** Immunostaining within the CA1 field. **d, f** Immunostaining within CA3. Neuronal expression of COX-2 in CA3 is widely seen among both nondemented subjects and AD patients. Although neuronal expression of COX-2 in CA1 is widespread in AD patients, it is less detectable among nondemented subjects. **c-f** Bars are 30 μm .

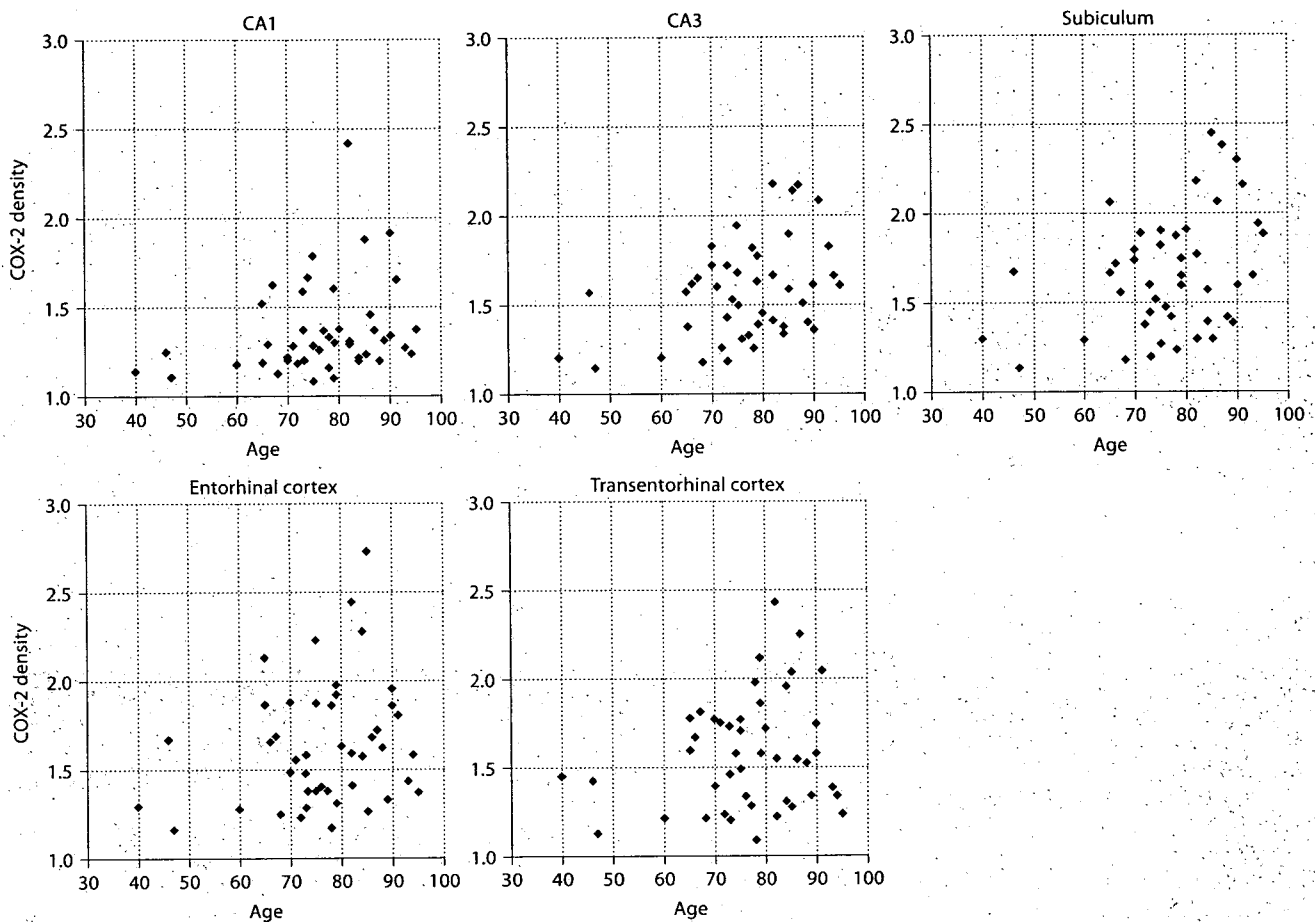


Fig. 3. A significant correlation exists between aging and COX-2 immunoreactivity in CA3 and the subiculum of nondemented subjects. In nondemented subjects, aging correlates with COX-2 immunoreactivity in CA3 and the subiculum (Pearson's correlation coefficient test, $r = 0.399$, $p = 0.007$; $r = 0.380$, $p = 0.010$, respectively).

sion of the hippocampus and subiculum of nondemented subjects, COX-2 immunoreactivity correlated with age (Pearson's correlation coefficient test, $r = 0.399$, $p = 0.007$; $r = 0.380$, $p = 0.010$, respectively) and this correlation was not evident in the CA1 subdivision of the hippocampus, entorhinal cortex or transentorhinal cortex (Pearson's correlation coefficient test, $r = 0.268$, $p = 0.078$; $r = 0.220$, $p = 0.147$; $r = 0.194$, $p = 0.202$, respectively).

Study B

Information of Nondemented Subjects and AD Patients

In study B, in order to compare the nondemented subjects with AD patients, we examined 25 nondemented subjects aged 76 years or more from study A and we col-

lected another 25 age- and sex-matched AD autopsy cases derived from Hisayama Town (table 1). All of the AD patients were free of other types of dementia.

COX-2 Immunoreactivity in the Hippocampus

The degrees of COX-2 immunoreactivity in different hippocampal subdivisions of nondemented subjects and AD patients are shown in figure 4. The immunoreactivity in CA1 was increased in AD patients as compared to nondemented subjects with high statistical significance (Mann-Whitney U test, $p = 0.001$; fig. 2c, e). On the other hand, the differences between the nondemented subjects and AD patients were small in CA3, subiculum, entorhinal cortex and transentorhinal cortex (Mann-Whitney U test, $p = 0.171$, $p = 0.467$, $p = 0.712$, $p = 0.621$,

Table 1. Subjects of study B

Nondemented subjects			Age- and sex-matched AD patients		
ID	Sex	Age	ID	Sex	Age
22735	F	76	23297	F	77
22907 ^C	F	77	21363	F	78
22880	F	78	22598	F	79
22939 ^C	M	78	23373	M	79
22739	F	79	23114	F	79
22910 ^C	F	79	23392	F	79
22819	M	79	20565	M	80
22803	M	80	23185	M	81
22933	M	82	20189	M	83
22828 ^C	F	82	20617	F	82
22892	M	82	20316	M	83
22772 ^C	F	84	20461	F	84
23015 ^C	F	84	22502	F	84
23061	M	85	20706	M	85
22906	F	85	23018	F	84
22950	F	86	20240	F	87
22795	M	87	21501	M	86
22976 ^C	F	88	23334	F	88
22798	M	89	22156	M	90
22767	F	90	20748	F	90
22992	F	90	23289	F	90
23021 ^C	M	91	23028	M	92
22955 ^C	F	93	23377	F	93
23055 ^C	F	94	22661	F	94
22896 ^C	F	95	23269	F	95

We studied all subjects aged >76 years of the 45 nondemented subjects of study A. As a comparison, we collected 25 age- and sex-matched AD patients. The subjects whose IDs are marked with 'C' are nondemented subjects with AD pathology (CERAD: moderate or frequent, with Braak and Braak stage 4, 5 or 6) and are the subjects of study C.

respectively). From these results, COX-2 immunoreactivity in CA1 has presumably been induced along with the development of AD; therefore, we assessed the influence of AD pathology on neuronal COX-2 expression in CA1.

COX-2 Immunoreactivity in CA1 Correlates with SP and NFT Density in AD Patients

In the CA1 subdivision of the hippocampi of AD patients, COX-2 immunoreactivity correlated with the semiquantification of SPs (Spearman's rank correlation test, $\rho = 0.500$, $p = 0.001$; fig. 5a) and with the number of NFTs (Pearson's correlation coefficient test, $r = 0.536$, $p = 0.003$; fig. 5b). On the other hand, in the CA1 subdivision of the hippocampi of nondemented subjects,

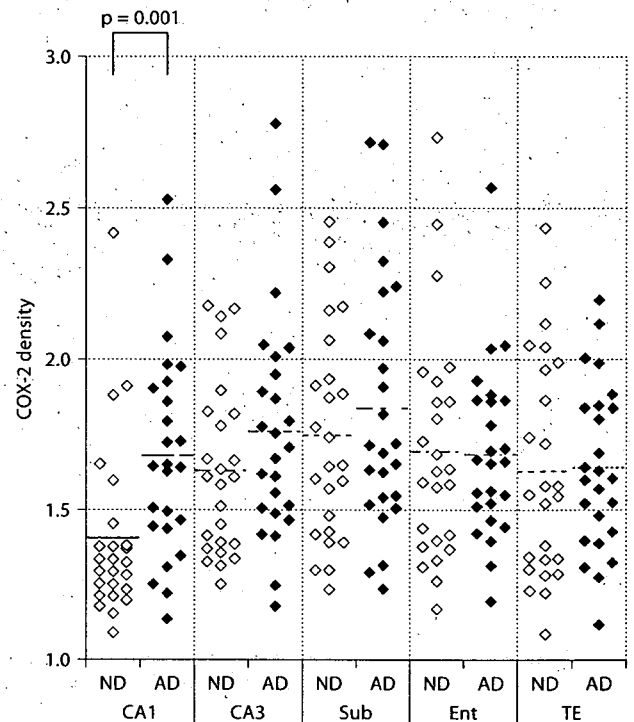


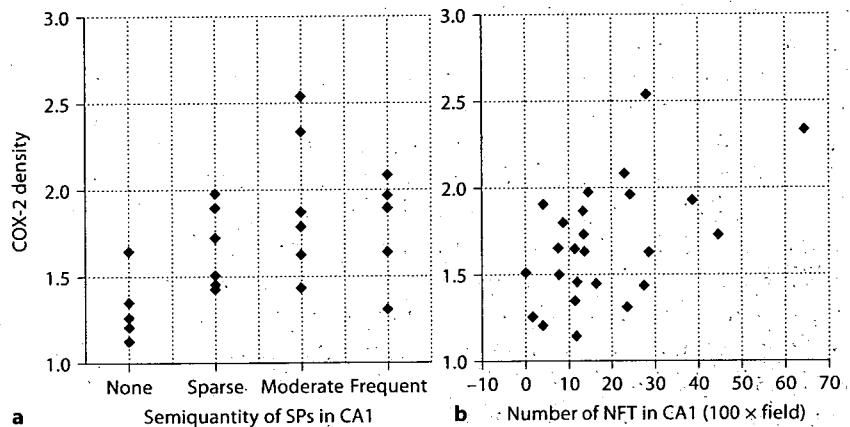
Fig. 4. Degrees of COX-2 immunoreactivity in different hippocampal subdivisions of nondemented subjects and AD patients. Immunoreactivity is increased in AD patients as compared to nondemented subjects, and the increase is observed in almost all hippocampal fields and reached statistical significance in the CA1 field (Mann-Whitney U test, $p = 0.001$). Bars represent the mean density of neurons in each area.

COX-2 immunoreactivity did not correlate with either the semiquantification of SPs (Spearman's rank correlation test, $\rho = 0.013$, $p = 0.949$) or the number of NFTs (Pearson's correlation coefficient test, $r = -0.141$, $p = 0.501$).

Study C

In the Hisayama study, we sometimes encountered autopsy cases that were cognitively normal though exhibited severe Alzheimer type pathology in their brains. Therefore, in study C, we compared the immunoreactivity of COX-2 in CA1 of 11 nondemented subjects with AD pathology (CERAD: moderate or frequent, with Braak and Braak stage 4, 5 or 6; table 1) with that of 11 age- and sex-matched AD patients. The immunoreactivity of COX-

Fig. 5. COX-2 immunoreactivity in CA1 correlates with SP (a) and NFT (b) density in AD patients. The semiquantitative density of SPs in CA1 was determined using guidelines established by CERAD. In AD patients, a correlation between COX-2 immunoreactivity and the semiquantitative density of SPs in CA1 was statistically significant (Spearman's rank correlation test, $\rho = 0.500$, $p = 0.001$). Also, a correlation between COX-2 immunoreactivity and the density of NFT in CA1 was statistically significant (Pearson's correlation coefficient test, $r = 0.536$, $p = 0.003$).



2 in CA1 of AD patients was obviously stronger than in nondemented subjects with AD pathology (Mann-Whitney U test, $p < 0.001$; fig. 6).

Discussion

To our knowledge, this is the first report that explores the regional distribution of COX-2 immunoreactivity in the hippocampi of nondemented subjects of a general population. We found that among nondemented subjects, COX-2 immunoreactivity in CA3, subiculum, entorhinal cortex and transentorhinal cortex was widespread, suggesting that COX-2 is constitutively expressed in these subdivisions of the hippocampus, whilst weak immunoreactivity was observed in CA1. In addition, in the CA3 subdivision of the hippocampi and subiculum of nondemented subjects, COX-2 immunoreactivity correlated with age, suggesting that the COX-2 expression in this region was augmented with aging in the normal condition.

Strong expression of COX-2 in the CA3 subdivision of the hippocampus and expression of COX-2 in the subiculum was reported previously in the normal rat brain [27]. Also, an immunohistochemical study of the human hippocampus showed more COX-2 positive neurons to be present in the CA3 than in the CA1 or CA2 field, and this difference became clearer when analysis was limited to dense staining [11]. These results are compatible with our data and indicate that our staining and assessment of COX-2 are reasonable and also suggest the constitutive expression of COX-2 in these subdivisions of the hippocampus.

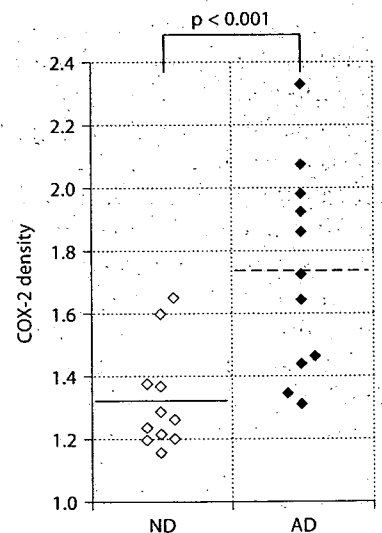


Fig. 6. Degrees of COX-2 immunoreactivity in the CA1 subdivision of the hippocampus of nondemented subjects with AD pathology and AD patients. COX-2 immunoreactivity is increased in AD patients as compared to nondemented subjects (Mann-Whitney U test, $p < 0.001$). Bars represent the mean density of neurons in each area.

The enhanced expression of COX-2 with age was reported in a study examining aged mouse macrophages [28], but little is known about changes in COX-2 expression in the human brain during aging. Now that several inflammatory processes are thought to play a critical role in brain aging and to be associated with an increased vul-

nerability to neurodegeneration [29], we think that our finding provides a new point of view in regard to the aging brain. For example, a COX inhibitor was reported to protect mice from age-associated cognitive impairment under normal conditions [30]. These studies may illustrate a new 'anti-aging' treatment for the human brain.

In addition, we assessed neuropathologically confirmed AD patients in order to appreciate the influence of AD pathology on COX-2 expression within the hippocampus. We found that COX-2 immunoreactivity was increased in AD patients as compared to nondemented subjects and this change was observed in almost all hippocampal fields, reaching statistical significance in the CA1 field. This difference remained statistically significant even when we limited the nondemented subjects to those with AD pathology. In other words, the upregulation of COX-2 in the CA1 field in conjunction with AD pathology may be one of the important factors for developing AD. Over the last 10 years, several studies have examined the expression of COX-2 in postmortem AD brain tissues but have yielded conflicting results. One of the problems in these studies is in the method of selecting the nondemented group used for comparison with the AD group. As we mentioned, there is a possibility that COX-2 expression may be augmented with age; therefore, in a study of aged subjects, the difference of COX-2 expression between the AD and the nondemented group may become small and the opposite may also be true. Making the matter complicated, the degree of this augmentation may differ in each area.

We found that COX-2 immunoreactivity in CA1 correlates with AD pathology in AD patients. A previous immunohistochemical study reported a similar result [8], and recently the possibility of a direct interaction between human A β and COX-2 being mediated by peroxidase activity was reported [31]. Why the correlation between COX-2 immunoreactivity in the CA1 field and AD

pathology was observed only in AD patients and not in nondemented subjects is still unclear and further examination is required.

Here, we assessed the relationship between the neuronal expression of COX-2 and AD. It has recently been reported that the neuronal expression of COX-2 may play an important role in other types of neurodegenerative disorders. For instance, neuronal COX-2 expression in all CA fields of the hippocampus was significantly upregulated in ALS patients as compared to control subjects [13] and COX-2 was upregulated in brain dopaminergic neurons of both Parkinson's disease and MPTP-treated mice [12]. Upregulation of neuronal COX-2 expression may be a common pathway that a variety of neurodegenerative disorders exhibit.

In conclusion, in this study we have explored the regional expression of COX-2 in the hippocampus of the normal brain, and based on this result we have also explored the correlation between AD pathology and COX-2 expression in this region. While COX-2 expression appears to be differently regulated amongst hippocampal subdivisions and its presence may be augmented with age in the cognitively normal brain, COX-2 expression within the CA1 field of AD brains may be associated with the cognitive decline to some extent.

Acknowledgments

This study was supported in part by a Grant in Aid for the 21st Century COE program and Grant in Aid for Scientists (No. 16300112) from the Ministry of Education, Culture, Sports, Science and Technology of Japan. We are grateful to Dr. Takeshi Iwatsubo, Department of Neuropathology and Neuroscience, University of Tokyo, for generously donating the α -synuclein antibody LB509. We thank Mr. S. Mawatari and Ms. S. Nagae for their technical assistance.

References

- 1 McGeer PL, Schulzer M, McGeer EG: Arthritis and anti-inflammatory agents as possible protective factors for Alzheimer's disease: a review of 17 epidemiologic studies. *Neurology* 1996;47:425-432.
- 2 Rogers J, Kirby LC, Hempelman SR, Berry DL, McGeer PL, Kaszniak AW, Zalinski J, Cofield M, Mansukhani L, Willson P, et al: Clinical trial of indomethacin in Alzheimer's disease. *Neurology* 1993;43:1609-1611.
- 3 Vane JR, Bakhle YS, Botting RM: Cyclooxygenases 1 and 2. *Annu Rev Pharmacol Toxicol* 1998;38:97-120.
- 4 Hoozemans JJ, Bruckner MK, Rozemuller AJ, Veerhuis R, Eikelenboom P, Arendt T: Cyclin D1 and cyclin E are co-localized with cyclo-oxygenase 2 (COX-2) in pyramidal neurons in Alzheimer disease temporal cortex. *J Neuropathol Exp Neurol* 2002;61:678-688.
- 5 Yasojima K, Schwab C, McGeer EG, McGeer PL: Distribution of cyclooxygenase-1 and cyclooxygenase-2 mRNAs and proteins in human brain and peripheral organs. *Brain Res* 1999;830:226-236.
- 6 Pect MG I, Horrobin DF: *Phospholipid Spectrum Disorder in Psychiatry*. Carnforth, Marius Press, 1999.
- 7 Ho L, Pieroni C, Winger D, Purohit DP, Aisen PS, Pasinetti GM: Regional distribution of cyclooxygenase-2 in the hippocampal formation in Alzheimer's disease. *J Neurosci Res* 1999;57:295-303.

- 8 Ho L, Purohit D, Haroutunian V, Luterma JD, Willis F, Naslund J, Buxbaum JD, Mohs RC, Aisen PS, Pasinetti GM: Neuronal cyclooxygenase 2 expression in the hippocampal formation as a function of the clinical progression of Alzheimer disease. *Arch Neurol* 2001;58:487-492.
- 9 Hoozemans JJ, Veerhuis R, Rozemuller AJ, Arendt T, Eikelenboom P: Neuronal COX-2 expression and phosphorylation of pRb precede p38 MAPK activation and neurofibrillary changes in AD temporal cortex. *Neurobiol Dis* 2004;15:492-499.
- 10 Oka A, Takashima S: Induction of cyclooxygenase 2 in brains of patients with Down's syndrome and dementia of Alzheimer type: specific localization in affected neurones and axons. *Neuroreport* 1997;8:1161-1164.
- 11 Yermakova AV, O'Banion MK: Downregulation of neuronal cyclooxygenase-2 expression in end stage Alzheimer's disease. *Neurobiol Aging* 2001;22:823-836.
- 12 Teismann P, Tieu K, Choi DK, Wu DC, Naini A, Hunot S, Vila M, Jackson-Lewis V, Przedborski S: Cyclooxygenase-2 is instrumental in Parkinson's disease neurodegeneration. *Proc Natl Acad Sci USA* 2003;100:5473-5478.
- 13 Yokota O, Terada S, Ishizu H, Ishihara T, Nakashima H, Kugo A, Tsuchiya K, Ikeda K, Hayabara T, Saito Y, Murayama S, Ueda K, Checler F, Kuroda S: Increased expression of neuronal cyclooxygenase-2 in the hippocampus in amyotrophic lateral sclerosis both with and without dementia. *Acta Neuropathol (Berl)* 2004;107:399-405.
- 14 Yokota O, Terada S, Ishihara T, Nakashima H, Kugo A, Ujike H, Tsuchiya K, Ikeda K, Saito Y, Murayama S, Ishizu H, Kuroda S: Neuronal expression of cyclooxygenase-2, a pro-inflammatory protein, in the hippocampus of patients with schizophrenia. *Prog Neuropsychopharmacol Biol Psychiatry* 2004;28:715-721.
- 15 Minghetti L: Cyclooxygenase-2 (COX-2) in inflammatory and degenerative brain diseases. *J Neuropathol Exp Neurol* 2004;63:901-910.
- 16 Katsuki S: Epidemiological and clinicopathological study on cerebrovascular disease in Japan. *Prog Brain Res* 1966;21:64-89.
- 17 Tanizaki Y, Kiyohara Y, Kato I, Iwamoto H, Nakayama K, Shinohara N, Arima H, Tanaka K, Ibayashi S, Fujishima M: Incidence and risk factors for subtypes of cerebral infarction in a general population: the Hisayama study. *Stroke* 2000;31:2616-2622.
- 18 Kiyohara Y, Yoshitake T, Kato I, Ohmura T, Kawano H, Ueda K, Fujishima M: Changing patterns in the prevalence of dementia in a Japanese community: the Hisayama study. *Gerontology* 1994;40:29-35.
- 19 Yoshitake T, Kiyohara Y, Kato I, Ohmura T, Iwamoto H, Nakayama K, Ohmori S, Nomiya K, Kawano H, Ueda K, et al: Incidence and risk factors of vascular dementia and Alzheimer's disease in a defined elderly Japanese population: the Hisayama Study. *Neurology* 1995;45:1161-1168.
- 20 Association AP: *Diagnostic and Statistical Manual of Mental Disorders*, ed 3, revised. Washington, American Psychiatric Association, 1987.
- 21 McKhann G, Drachman D, Folstein M, Katzman R, Price D, Stadlan EM: Clinical diagnosis of Alzheimer's disease: report of the NINCDS-ADRDA Work Group under the auspices of Department of Health and Human Services Task Force on Alzheimer's Disease. *Neurology* 1984;34:939-944.
- 22 Mirra SS, Heyman A, McKeel D, Sumi SM, Crain BJ, Brownlee LM, Vogel FS, Hughes JP, van Belle G, Berg L: The Consortium to Establish a Registry for Alzheimer's Disease (CERAD). II. Standardization of the neuropathologic assessment of Alzheimer's disease. *Neurology* 1991;41:479-486.
- 23 McKeith IG, Dickson DW, Lowe J, Emre M, O'Brien JT, Feldman H, Cummings J, Duda JE, Lippa C, Perry EK, Aarsland D, Arai H, Ballard CG, Boeve B, Burn DJ, Costa D, Del Ser T, Dubois B, Galasko D, Gauthier S, Goetz CG, Gomez-Tortosa E, Halliday G, Hansen LA, Hardy J, Iwatsubo T, Kalaria RN, Kaufer D, Kenny RA, Korczyn A, Kosaka K, Lee VM, Lees A, Litvan I, Lodos E, Lopez OL, Minoshima S, Mizuno Y, Molina JA, Mukaetova-Ladinska EB, Pasquier F, Perry RH, Schulz JB, Trojanowski JQ, Yamada M: Diagnosis and management of dementia with Lewy bodies: third report of the DLB Consortium. *Neurology* 2005;65:1863-1872.
- 24 Baba M, Nakajo S, Tu PH, Tomita T, Nakaya K, Lee VM, Trojanowski JQ, Iwatsubo T: Aggregation of alpha-synuclein in Lewy bodies of sporadic Parkinson's disease and dementia with Lewy bodies. *Am J Pathol* 1998;152:879-884.
- 25 Braak H, Alafuzoff I, Arzberger T, Kretschmar H, Del Tredici K: Staging of Alzheimer disease-associated neurofibrillary pathology using paraffin sections and immunocytochemistry. *Acta Neuropathol (Berl)* 2006;112:389-404.
- 26 Anonymous: Consensus recommendations for the postmortem diagnosis of Alzheimer's disease. The National Institute on Aging, and Reagan Institute Working Group on Diagnostic Criteria for the Neuropathological Assessment of Alzheimer's Disease. *Neurobiol Aging* 1997;18:S1-S2.
- 27 Breder CD, Dewitt D, Kraig RP: Characterization of inducible cyclooxygenase in rat brain. *J Comp Neurol* 1995;355:296-315.
- 28 Hayek MG, Mura C, Wu D, Beharka AA, Han SN, Paulson KE, Hwang D, Meydani SN: Enhanced expression of inducible cyclooxygenase with age in murine macrophages. *J Immunol* 1997;159:2445-2451.
- 29 Uz T, Pesold C, Longone P, Manev H: Aging-associated up-regulation of neuronal 5-lipoxygenase expression: putative role in neuronal vulnerability. *FASEB J* 1998;12:439-449.
- 30 Bishnoi M, Patil CS, Kumar A, Kulkarni SK: Protective effects of nimesulide (COX inhibitor), AKBA (5-LOX inhibitor), and their combination in aging-associated abnormalities in mice. *Methods Find Exp Clin Pharmacol* 2005;27:465-470.
- 31 Nagano S, Huang X, Moir RD, Payton SM, Tanzi RE, Bush AI: Peroxidase activity of cyclooxygenase-2 (COX-2) cross-links beta-amyloid (Abeta) and generates Abeta-COX-2 hetero-oligomers that are increased in Alzheimer's disease. *J Biol Chem* 2004;279:14673-14678.

プリオン病への治療アプローチ*

堂浦 克美**

Key Words : prion disease, therapy, pentosan polysulphate, amyloidophilic chemical, prion imaging

変異型プリオン病や医原性プリオン病（下垂体ホルモン製剤やヒト乾燥硬膜の使用による）が若年者で多発し、プリオン病の治療開発への関心が高まっている。しかしながら、患者および発症リスクキャリアーの数は製薬企業に創薬への関心を抱かせるほど多くはなく、プリオン病の治療開発は医者や医学・薬学研究者に委ねられている。

プリオン病は、蛋白質性感染因子であるプリオンが原因で起こる病気であり、プリオンの本体は異常型プリオン蛋白である。この蛋白は難溶性で凝集体を形成し、脳に沈着する。プリオン病治療の標的は、この異常型プリオン蛋白の産生を抑制すること、異常型プリオン蛋白の分解を促進すること、異常型プリオン蛋白による神経変性を抑えることである（Fig. 1）。細菌やウイルスなどの通常病原因子と異なり核酸を持たないプリオンがどのように増殖複製するのか、その機序解明はいまだにプリオン病研究の中で最も魅力的な研究テーマの一つであるため、異常型プリオン蛋白の産生阻害メカニズムに関する研究や阻害化合物の探索研究は活発に展開されている。この領域においては、遺伝子治療や再生医療などを見据えた基礎研究も進められているが、これまでにインビボ実験で目を見張るような成果は得られていない。一

方、阻害化合物を基にした創薬研究も活発に進められ、インビボ実験でも有効なものが発見されるようになっているが、ヒトへの応用にはなお5年、10年といった時間を要する段階にある。

これらの治療法開発研究や創薬研究と並行して、即戦的な治療薬探索研究も行われている。これは、他の疾患の治療に使われている医薬品の中からプリオン病治療に応用できるものを探索するものである。これまでにマラリアの治療薬であるquinacrineやquinine^{1,2)}、非麻薬性鎮痛剤であるflupirtine³⁾、間質性膀胱炎や静脈炎の治療薬であるpentosan polysulphate⁴⁾、抗生物質であるdoxycycline⁵⁾、高脂血症の治療薬であるsimvastatin⁶⁾などに治療効果が観察されている。Quinacrine, quinine, pentosan polysulphate, simvastatinは異常型プリオン蛋白の産生抑制に、doxycyclineは異常型プリオン蛋白の分解促進に、flupirtine, simvastatinは神経変性抑制に働いている。Quinacrine, quinine, flupirtineはすでに患者で実験的治療が実施されて、効果と安全性についての評価が行われた。Quinacrineやquinineは、一過性の脳機能改善効果が患者で観察されたが、肝障害などの副作用が高率に発生したため、現在のところ積極的には患者への投与は行われていな

* Therapeutic Approaches to Prion Diseases.

** 東北大学大学院医学系研究科プリオン蛋白分子解析分野 Katsumi DOH-URA : Department of Prion Research, Tohoku University Graduate School of Medicine

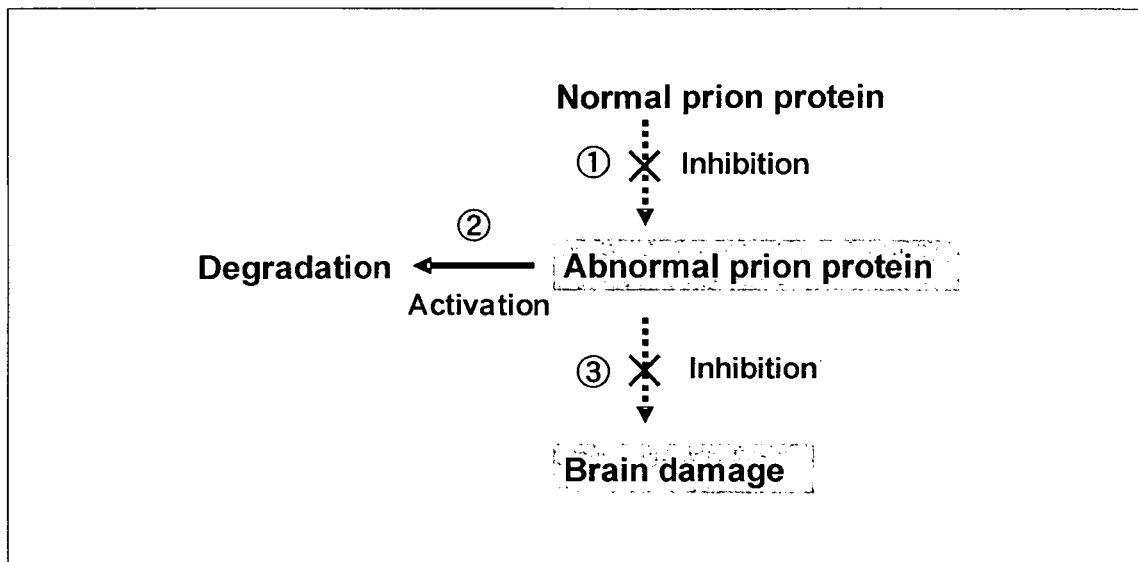


Fig. 1 Potential drug targets for the treatment of prion diseases

Inhibition of abnormal prion protein synthesis (①), activation of abnormal prion protein degradation (②), and inhibition of brain damage caused by abnormal prion protein (③) are potential drug targets.

い⁷⁾。Flupirtineは、患者の認知機能障害の改善に有効であるが、生命予後を改善する効果はないことが明らかとなっている⁸⁾。一方、doxycyclineやsimvastatinは、イタリアとドイツで患者への実験的治療が始まっており、国内においても、これらの医薬品を使った実験的治療の準備が進められている。Pentosan polysulphateは英国、フランス、米国、日本の患者で実験的治療が実施されているところであり、次に記載するように効果と安全性について評価が行われている。

Pentosan polysulphateの脳室内持続投与は、我々がその優れた治療効果を動物実験で発見し安全性を確認した実験的治療法である⁹⁾。この治療法はこれまでに25例のプリオン病患者で実施されている。亜急性に進行するプリオン病では効果はなく、変異型ヤコブ病のように緩徐進行型プリオン病の若年発症者で延命効果が期待されるが、病気の進行を完全に止めてしまう程の治療効果は得られていない^{9,10)}。また、長期治療中に硬膜下水腫を合併する症例が比較的多く、その原因は不明である。日本では、緩徐に進行する病型のプリオン病患者において、効果と安全性の評価が続けられている。Pentosan polysulphate療法は脳神経外科手術を必要とする侵襲的な治療法であり、

脳室カテーテルや持続注入ポンプの留置手術を必要とする点だけでなく、pentosan polysulphateの脳室から脳実質内への拡散が効率的でない点、pentosan polysulphateが弱い抗凝血作用を持っている点などが弱点となっている。末梢投与で本治療法の効果を凌ぐ治療薬の開発が必要である。

一方、我々はアミロイド親和性化合物が抗プリオン活性を持っていることをこれまで報告してきた^{11,12)}。アミロイド親和性化合物はAlzheimer病の新規画像診断薬（アミロイド・イメージングプローブ）として最近盛んに開発されている¹³⁾。脳移行性に優れたアミロイド・イメージング化合物は、プリオン感染動物の末梢静脈内に投与した場合には脳内のプリオン・アミロイドを描出できるだけでなく、生命予後改善効果を発揮する。我々が最近発見したアミロイド親和性化合物は、経口投与でも良好な脳移行を示し、プリオン感染マウスにおいて優れた生命予後改善効果を発揮するものである¹⁴⁾。この化合物は、プリオン感染マウスで治療効果を発揮するだけでなく、Alzheimer病モデルマウスにおいても老人斑沈着を抑制するなどの治療効果を発揮し、脳内にアミロイド沈着を起こす疾患の治療に有効と考えられる。このアミロイド親和性化合物をヒトに応用するには安全性

や治療効果を上げるために物性を改良する必要があり、創薬のプロである製薬企業の協力なしには実用化は困難である。市場性のないプリオン病治療薬開発に製薬企業を巻き込むためには、市場性のある疾患の治療薬開発とリンクさせることが一つの手段と考えられ、アミロイド親和性化合物がその一例として期待される。

動物実験では感染の極早期から治療を開始すれば、より一層の生命予後改善効果が観察されることより、早期診断（特に発症前診断）開発は治療開発とともにプリオン病を克服する上で必要不可欠である。また、病勢や治療効果を評価するための手段の開発も必要不可欠である。これまでは、罹病期間が治療効果の評価指標として一般的に使われてきたが、罹病期間は発症年齢、性別、病型、看護・介護、延命治療などにより影響を受けるため良い指標とは言えない。患者の脳内のプリオンを直接測定することが出来ないことや、早期診断・病勢診断の指標となる良い代理マーカーがないことが問題である。我々は、患者の脳内に蓄積した異常プリオン蛋白をアミロイド親和性化合物をプローブとしてPET（ポジトロン・エミッション・トモグラフィ）で画像化できないか検討を開始した。脳内に蓄積した異常プリオン蛋白量をイメージングで測定できれば、信頼性の高い早期診断・病勢診断や治療効果の評価が可能となる。

文 献

- 1) Doh-Ura K, Iwaki T, Caughey B : Lysosomotropic agents and cysteine protease inhibitors inhibit scrapie-associated prion protein accumulation. *J Virol* 74 : 4894-4897, 2000
- 2) Murakami-Kubo I, Doh-Ura K, Ishikawa K et al : Quinoline derivatives are therapeutic candidates for transmissible spongiform encephalopathies. *J Virol* 78 : 1281-1288, 2004
- 3) Schroder HC, Muller WE : Neuroprotective effect of flupirtine in prion disease. *Drugs Today* 38 : 49-58, 2002
- 4) Doh-ura K, Ishikawa K, Murakami-Kubo I et al : Treatment of transmissible spongiform encephalopathy by intraventricular drug infusion in animal models. *J Virol* 78 : 4999-5006, 2004
- 5) Forloni G, Iussich S, Awan T et al : Tetracyclines affect prion infectivity. *Proc Natl Acad Sci USA* 99 : 10849-10854, 2002
- 6) Mok SW, Thelen KM, Riemer C et al : Simvastatin prolongs survival times in prion infections of the central nervous system. *Biochem Biophys Res Commun* 348 : 697-702, 2006
- 7) 山田達夫, 坪井義夫, 中島雅士ほか : クロイツフェルト・ヤコブ病患者における抗マラリア薬, キナクリン, キニーネ治療の効果と副作用に関する研究. 厚生科学研究費補助金(こころの健康科学研究事業)「即戦略的クロイツフェルト・ヤコブ病治療法の確立に関する研究」(主任研究者 堂浦克美) 平成15年度総括研究報告書, p11-22, 平成16年4月
- 8) Otto M, Cepek L, Ratzka P et al : Efficacy of flupirtine on cognitive function in patients with CJD : A double-blind study. *Neurology* 62 : 714-718, 2004
- 9) Parry A, Baker I, Stacey R et al : Long term survival in a patient with variant Creutzfeldt-Jakob disease treated with intraventricular pentosan polysulphate. *J Neurol Neurosurg Psychiatry* 78 : 733-734, 2007
- 10) Rainov NG, Tsuboi Y, Krolak-Salmon P et al : Experimental treatments for human transmissible spongiform encephalopathies : is there a role for pentosan polysulfate? *Expert Opin Biol Ther* 7 : 713-726, 2007
- 11) Ishikawa K, Doh-ura K, Kudo Y et al : Amyloid imaging probes are useful for detection of prion plaques and treatment of transmissible spongiform encephalopathies. *J Gen Virol* 85 : 1785-1790, 2004
- 12) Ishikawa K, Kudo Y, Nishida N et al : Styrylbenzazole derivatives for imaging of prion plaques and treatment of transmissible spongiform encephalopathies. *J Neurochem* 99 : 198-205, 2006
- 13) Furumoto S, Okamura N, Iwata R et al : Recent advances in the development of amyloid imaging agents. *Curr Top Med Chem* 7 : 1773-1789, 2007
- 14) Kawasaki Y, Kawagoe K, Chen CJ et al : Orally administered amyloidophilic compound is effective in prolonging the incubation periods of animals cerebrally infected with prion diseases in a prion strain-dependent manner. *J Virol* 81 : 12889-12898, 2007